

Vascular System Defects and Impaired Cell Chemokinesis as a Result of $G\alpha_{13}$ Deficiency

Stefan Offermanns, Valeria Mancino,
Jean-Paul Revel, Melvin I. Simon

Heterotrimeric GTP-binding proteins (G proteins) participate in cellular signaling and regulate a variety of physiological processes. Disruption of the gene encoding the G protein subunit α_{13} ($G\alpha_{13}$) in mice impaired the ability of endothelial cells to develop into an organized vascular system, resulting in intrauterine death. In addition, $G\alpha_{13}$ ($-/-$) embryonic fibroblasts showed greatly impaired migratory responses to thrombin. These results demonstrate that $G\alpha_{13}$ participates in the regulation of cell movement in response to specific ligands, as well as in developmental angiogenesis.

G proteins are signal transducers that couple a variety of receptors to effectors such as enzymes and ion channels (1). Heterotrimeric G proteins consist of an α , β , and γ subunit and are defined by the identity of their α subunit. Sixteen α -subunit genes have been cloned, and on the basis of sequence similarities they can be divided into four families ($G\alpha_s$, $G\alpha_{i/o}$, $G\alpha_q$, and $G\alpha_{12}$) (2). Whereas considerable knowledge exists about the cellular function of most members of the $G\alpha_s$, $G\alpha_{i/o}$, and $G\alpha_q$ families, the cellular and biological functions of G_{12} and G_{13} (which constitute the G_{12} family) are not known. The α subunit of G_{13} is expressed ubiquitously and shows 67% amino acid identity to $G\alpha_{12}$ (3). Studies with constitutively activated forms of $G\alpha_{13}$ have provided evidence that it may participate in the regulation of the Jun kinase/stress-activated protein kinase pathway (4), the Na^+/H^+ exchanger, and the Rho-dependent formation of stress fibers (5, 6).

To elucidate its biological function, we have disrupted the gene encoding $G\alpha_{13}$ ($Gna-13$) by homologous recombination in embryonic stem (ES) cells (Fig. 1). Germ-line-transmitting chimeric mice were generated with two independently targeted ES cell clones, and the targeted mutation of the $G\alpha_{13}$ gene was crossed into inbred (129/Sv) and outbred backgrounds (C57BL/6J). Mice heterozygous for the targeted mutation appeared normal and showed no obvious defects over an 18-month period. However, no homozygous $G\alpha_{13}$ mutant mice were found among 451 newborn animals from intercrosses between heterozygous mice. The ratio of wild-type to heterozygous offspring was 1:1.93, indicating a recessive lethal phenotype.

To determine the time at which the $G\alpha_{13}$ deficiency was manifest, we examined embryos from heterozygous intercrosses at

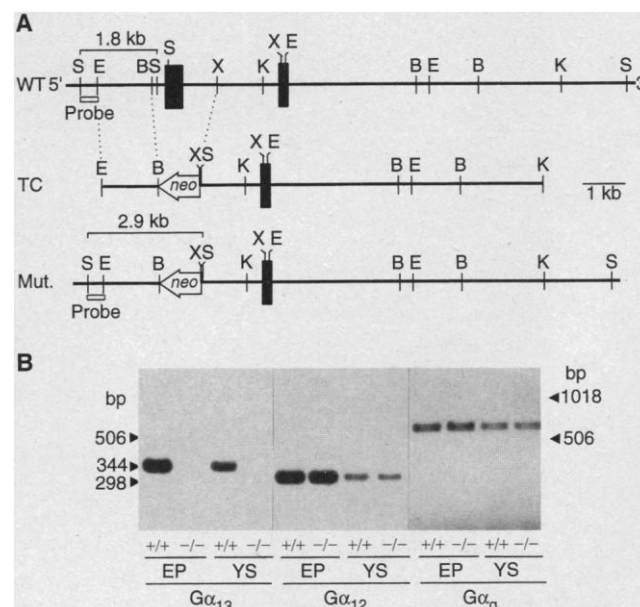
different developmental stages. Homozygous embryos were mostly resorbed by embryonic day 10.5 (E10.5), but could be recovered at E9.5 with hearts still beating. E9.5 homozygous mutants [detected by Southern (DNA) blotting or polymerase chain reaction] were poorly developed and misshapen compared to wild-type embryos (Fig. 2, C and D) and represented about 25% of all embryos at this stage. E8.5 $G\alpha_{13}$ ($-/-$) embryos, in contrast, appeared to be normal (Fig. 2, A and B). The phenotypes of homozygous $G\alpha_{13}$ mutant embryos were indistinguishable in inbred and outbred genetic backgrounds as well as in mouse lines derived from two independent ES cell clones.

We examined the expression of the $G\alpha_{13}$ gene by means of reverse transcription-polymerase chain reaction (RT-PCR) with total RNA prepared from wild-type

and mutant E8.5 embryos. The results (Fig. 1B) demonstrate the expression of $G\alpha_{13}$ both in the embryo proper and in the yolk sac of wild-type embryos but not in mutant embryos. Two other G protein α subunits, $G\alpha_{12}$ and $G\alpha_q$, were expressed both in mutant and wild-type embryos (Fig. 1B). Whole-mount in situ hybridization indicated that $G\alpha_{13}$ was expressed ubiquitously in E8.5 and E9.5 wild-type embryos, whereas no expression was detected in homozygous mutant embryos. $G\alpha_{12}$, similarly, showed ubiquitous expression in E8.5 and E9.5 wild-type embryos but was also expressed in $G\alpha_{13}$ homozygous mutant embryos (7). Ubiquitous expression suggests that $G\alpha_{13}$ might play a role in basic cellular function, whereas the apparently normal development of the embryo until E8 to E8.5 suggests that the absence of $G\alpha_{13}$ gene function did not have an acute effect until a specific developmental stage was induced.

The first obvious morphological defect in $G\alpha_{13}$ homozygous mutant embryos was present in the yolk sac, which starting from E8.5 appeared opaque and roughened compared to wild-type yolk sacs and developed no visible blood vessels. We visualized the vascular endothelial cells in wild-type and mutant yolk sacs in whole mount with monoclonal antibodies to PECAM-1 (anti-PECAM-1), which serve as a marker for differentiated endothelial cells (8). In E8.5 mutant yolk sacs, differentiated endothelial cells were present but did not form the organized honeycombed array seen in wild-type yolk sacs (Fig. 2, E and F). In normal development, between E8.5 and E9.5 endothelial cells reorganize into a vascular net-

Fig. 1. Targeted disruption of the murine $G\alpha_{13}$ gene. (A) Part of the wild-type $G\alpha_{13}$ locus containing the first and second exon (WT), the targeting construct (TC), and the targeted locus (Mut.) are shown. The $G\alpha_{13}$ gene was disrupted by means of a targeting vector in which a Bam HI-Xho I fragment containing the first exon was replaced by the neomycin resistance (*neo*) gene (22). The sizes of the Sma I fragments predicted to hybridize to the indicated diagnostic probe are shown. Restriction endonucleases: B, Bam HI; E, Eco RI; K, Kpn I; S, Sma I; and X, Xho I. (B) RT-PCR analysis of $G\alpha$ expression. Total RNA was prepared from E8.5 mutant and wild-type yolk sacs (YS) and from the embryo proper (EP) and used for RT-PCR analysis with $G\alpha_{13}$ -, $G\alpha_{12}$ -, and $G\alpha_q$ -specific primers hybridizing to regions encoded by different exons (23).



Division of Biology 147-75, California Institute of Technology, Pasadena, CA 91125, USA.

work that feeds into the embryo proper. E9.5 mutant yolk sacs, however, showed no vascular structures and appeared to contain fewer endothelial cells (Fig. 2, G and H). The degeneration of the yolk sac vascular system resulted in the separation of the mesodermal and endodermal layers of the yolk sac with the occasional presence of hematopoietic cells, whereas blood islands containing hematopoietic cells were readily apparent at this stage between the closely attached layers in the wild-type yolk sac (Fig. 3, A and B).

Similar defects in organization of the vascular system were observed in the embryo proper. The head mesenchyme of E8.5

mutant embryos contained enlarged blood vessels instead of the small vessels found in wild-type or heterozygous embryos (Fig. 3, C and D). The endothelial cell layer was at some places defective, resulting in leakage of blood cells into the mesenchyme. The heart and dorsal aortas appeared to be normal. In contrast, the E9.5 mutant embryos were dystrophic and cell death was observed throughout the embryo, especially in the neuroepithelium. Blood vessels of the head mesenchyme were extremely enlarged and highly disorganized; they were lined by endothelial cells and contained some nucleated blood cells (Fig. 3F). Blood vessels were also found at abnormal locations, such as

the space between the surface ectoderm and the neuroepithelium (Fig. 3G). Sporadic discontinuities of the endothelial layer resulted from a lack of cell integrity rather than from defective cell junctions that appeared to be normal at high magnification (Fig. 3, H and I). We conclude that $G\alpha_{13}$ homozygous mutant embryos die because of a failure to develop a functional vascular system.

Blood vessel formation during embryonic development is mediated by two processes: vasculogenesis (the differentiation of endothelial cells from progenitor cells) and angiogenesis (the subsequent growth and sprouting of endothelial cells, which gives

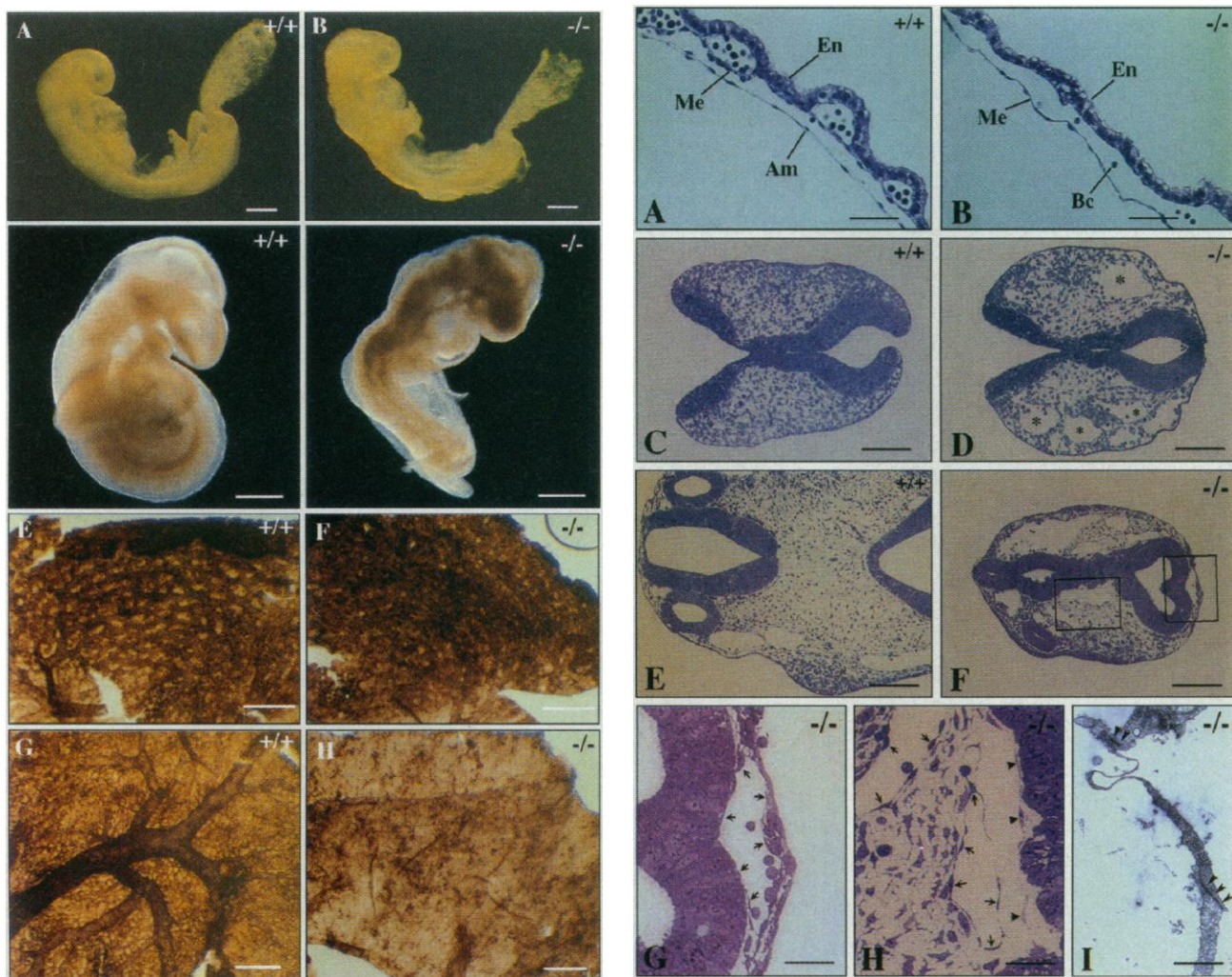


Fig. 2 (left). $G\alpha_{13}$ mutant phenotype. (A and B) Side view of wild-type (A) and mutant E8.5 embryos (B). (C and D) Side view of wild-type (C) and mutant E9.5 embryos (D). (E to H) Whole mount immunohistostaining of wild-type (E and G) and mutant yolk sacs (F and H) from E8.5 (E and F) and E9.5 embryos (G and H) with anti-PECAM-1 (24). Bars: 250 μ m (A and B), 500 μ m (C and D), 350 μ m (E and F), and 650 μ m (G and H). **Fig. 3 (right).** Vascular system defects in $G\alpha_{13}$ mutant embryos. (A and B) Hematoxylin-eosin-stained sections through E9.0 wild-type (A) and mutant yolk sac (B). Am, amnion; Bc, blood cell; En, extraembryonic endoderm; Me, extraembryonic mesoderm. (C and D) Toluidin blue-stained transverse Epon sections through heads of wild-type (C) and mutant E8.5 embryos (D) showing en-

larged blood vessels in the head mesenchyme of $G\alpha_{13}$ -deficient embryos (asterisks). (E and F) Toluidin blue-stained transverse Epon sections through heads of wild-type (E) and mutant E9.5 embryos (F). (G and H) Magnified areas from transverse section through head of mutant E9.5 embryo showing abnormal location of blood vessel between embryonic ectoderm and neuroepithelium of the mesencephalon (G) as well as defective blood vessels (H). Arrows point to endothelial cells; arrowheads mark degenerated endothelial-like cells. (I) Ultrastructural analysis of endothelial cells from E9.5 mutant embryos. Arrowheads point to junctions between individual endothelial cells (25). Bars: 60 μ m (A and B), 120 μ m (C and D), 170 μ m (E and F), 40 μ m (G and H), and 0.9 μ m (I).

rise to the organized vascular system) (9). The lack of $G\alpha_{13}$ did not affect the differentiation of progenitor cells into endothelial cells, which were apparent throughout the embryo. Rather, defects occurred during the subsequent process of angiogenesis, which includes sprouting, growth, migration, and remodeling of endothelial cells. The vascular system defects at E8.5 were most apparent in the extraembryonic vessels and in the vessels of the head mesenchyme. The head mesenchyme is probably vascularized by angiogenesis through migration of angioblasts rather than by in situ differentiation of endothelial cells (10). Examination of the molecular signaling processes that regulate vascular system development has so far focused mainly on receptor tyrosine kinases and cell adhesion molecules. Both systems play important roles in vasculogenic and angiogenic processes (9,

11–13). The phenotype of $G\alpha_{13}$ -deficient mice demonstrates that G protein-mediated signal transduction processes are also involved in angiogenesis.

To examine possible defects in responses to extracellular stimuli, we cultured fibroblastlike cells from E8.5 embryos as described (13). $G\alpha_{13}$ ($-/-$) cells were morphologically indistinguishable from wild-type cells and attached well to fibronectin and polylysine. Thrombin, whose receptor couples to $G\alpha_{13}$ (14), bradykinin, and lysophosphatidic acid (LPA), increased the production of inositol phosphates in wild-type and mutant cells, indicating that both cell types expressed appropriate G protein-coupled receptors (Fig. 4A). Similarly, mitogenic effects of thrombin, LPA, and fetal calf serum (FCS) were not significantly different in wild-type and $G\alpha_{13}$ -deficient cells (Fig. 4B). Whereas in wild-type cells, thrombin, fibronectin, and FCS (7) caused an increase in cell migration, in $G\alpha_{13}$ -deficient cells, the effect of thrombin was almost completely abrogated (Fig. 4C). Cell migration is a complex integrated process that involves the organized polymerization of actin filaments and the regulated formation of adhesive complexes (15). Cdc42, Rac, and Rho, all members of the Rho family of small molecular weight G proteins, participate in the regulation of these processes by extracellular factors (16). An activated form of $G\alpha_{13}$ induces cytoskeletal changes by way of Rho and activates Na^+/H^+ exchange in a RhoA- and Cdc42-dependent manner (5, 6). However, other G proteins—including G_i and G_{12} , which are expressed in embryonic fibroblasts (7) and are activated by thrombin receptors (14)—have been implicated in the regulation of cytoskeletal organization or cell motility (6, 17). We have shown that preincubation of embryonic fibroblasts with pertussis toxin, which uncouples G_i -type G proteins from receptors, resulted in a 50% reduction in migration of wild-type cells in response to thrombin (7). Thus, our data suggest that $G\alpha_{13}$ is required for the full migratory response to certain stimuli, but is probably not the only G protein involved in G protein-mediated regulation of cell movement.

We speculate that a failure of local cell movement and orientation in response to specific extracellular stimuli is a cellular mechanism underlying the observed vascular system defects in $G\alpha_{13}$ ($-/-$) embryos. The observed defects suggest that $G\alpha_{13}$ and its closest relative, $G\alpha_{12}$, fulfill at least partially nonoverlapping cellular and biological functions. In the adult organism, new vessels are formed only through angiogenesis, and adult angiogenesis with few exceptions is confined to pathological situations like wound healing

and tumor angiogenesis, which is important for the growth of solid tumors (18). The continued expression of $G\alpha_{13}$ and its role in developmental angiogenesis suggest that G protein-mediated signaling events involving $G\alpha_{13}$ may also be important in these pathological processes.

REFERENCES AND NOTES

1. J. R. Hepler and A. G. Gilman, *Trends Biochem. Sci.* **17**, 383 (1992); L. Birnbaumer, *Cell* **71**, 1068 (1992); A. M. Spiegel, A. Shenker, L. S. Weinstein, *Endocr. Rev.* **13**, 536 (1992); E. J. Neer, *Cell* **80**, 249 (1995).
2. M. I. Simon, M. P. Strathmann, N. Gautam, *Science* **252**, 802 (1991).
3. M. P. Strathmann and M. I. Simon, *Proc. Natl. Acad. Sci. U.S.A.* **88**, 5582 (1991).
4. M. V. S. Varas Prasad, J. M. Dermott, L. E. Heasley, G. L. Johnson, N. Dhanasekaran, *J. Biol. Chem.* **270**, 18655 (1995).
5. T. Voinno-Yasenetskaya et al., *ibid.* **269**, 4721 (1994); N. Dhanasekaran, M. V. S. Varas Prasad, S. J. Wadsworth, J. M. Dermott, G. van Rossum, *ibid.*, p. 11802; R. Hooley, C.-Y. Yu, M. Symons, D. L. Barber, *ibid.* **271**, 6152 (1996).
6. A. M. Buhl, M. L. Johnson, N. Dhanasekaran, G. L. Johnson, *ibid.* **270**, 24631 (1995).
7. S. Offermanns and M. I. Simon, unpublished data.
8. A. Vecchi et al., *Eur. J. Cell Biol.* **63**, 247 (1994); H. S. Baldwin et al., *Development* **120**, 2539 (1994).
9. W. Risau and I. Flamme, *Annu. Rev. Cell Dev. Biol.* **11**, 73 (1995).
10. D. M. Noden, in *The Development of the Vascular System*, R. N. Feinberg, G. K. Sherer, R. Auerbach, Eds. (Karger, Basel, 1991), pp. 1–24.
11. F. Shalaby et al., *Nature* **376**, 62 (1995); G.-H. Fong, J. Rossant, M. Gertsenstein, M. L. Breitman, *ibid.*, p. 66; T. N. Sato et al., *ibid.*, p. 70; M. Henkemeyer et al., *ibid.* **377**, 695 (1995); P. Carmeliet et al., *ibid.* **380**, 435 (1996); N. Ferrara et al., *ibid.*, p. 439.
12. E. L. George, E. N. Georges-Labouesse, R. S. Patel-King, H. Rayburn, R. O. Hynes, *Development* **119**, 1079 (1993).
13. J. T. Yang, H. Rayburn, R. O. Hynes, *ibid.*, p. 1093.
14. S. Offermanns, K. L. Laugwitz, K. Spicher, G. Schultz, *Proc. Natl. Acad. Sci. U.S.A.* **91**, 504 (1994).
15. B. M. Gumbiner, *Cell* **84**, 345 (1996); D. A. Lauffenburger and A. F. Horwitz, *ibid.*, p. 359.
16. C. D. Nobes and A. Hall, *ibid.* **81**, 53 (1995); L. M. Machesky and A. Hall, *Trends Cell Biol.* **6**, 304 (1996); S. H. Zigmond, *Curr. Opin. Cell Biol.* **8**, 66 (1996); S. W. Craig and R. P. Johnson, *ibid.*, p. 74.
17. M. W. Verghese, L. Charles, L. Jakoi, S. B. Dillon, R. Snyderman, *J. Immunol.* **138**, 4374 (1987); S. Sozani et al., *ibid.* **147**, 2215 (1991); G. Sa and P. L. Fox, *J. Biol. Chem.* **269**, 3219 (1994); M. A. del Pozo, P. Sánchez-Mateos, M. Nieto, F. Sánchez-Madrid, *J. Cell Biol.* **131**, 495 (1995).
18. J. Folkman, *Nature Med.* **1**, 27 (1995); D. Hanahan and J. Folkman, *Cell* **86**, 353 (1996).
19. R. Ramírez-Solis, A. N. Davis, A. Bradley, *Methods Enzymol.* **225**, 855 (1993).
20. C. Davis, *ibid.*, p. 502.
21. S. Offermanns and M. I. Simon, *J. Biol. Chem.* **270**, 15175 (1995); T. Higgins and E. Rozengurt, in *Cell Biology, A Laboratory Handbook*, J. E. Celis, Ed. (Academic Press, San Diego, 1994), pp. 294–301.
22. Using a probe representing base pairs 1 to 793 of the murine $G\alpha_{13}$ cDNA, we isolated a genomic clone from a 129/Sv mouse genomic λ phage library (Stratagene). The genomic clone used for gene targeting contained the first two exons of the $G\alpha_{13}$ gene. To generate a null mutation, we replaced a 1.5-kb Bam HI to Xho I fragment containing the first exon by the *neo* gene from plasmid pMC1neo Poly A (Stratagene). The targeting vector contained 1.4 kb upstream sequence as the 5' arm and 8 kb of intron sequence and second exon as the 3' arm. A Sma I site was introduced between the long arm of the construct and the *neo* cassette. Gene targeting in the

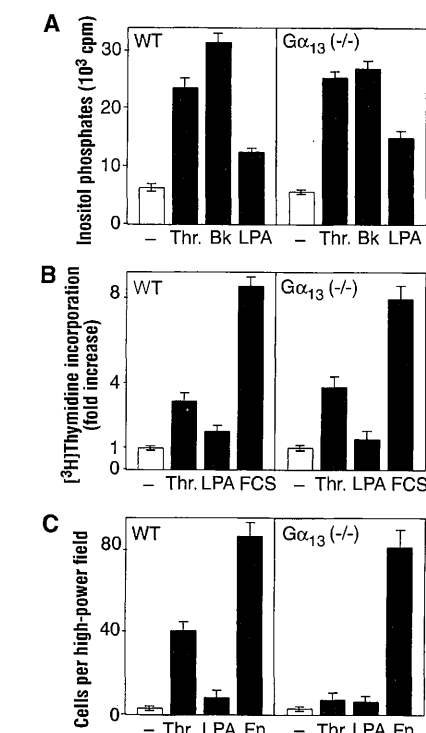


Fig. 4. Phenotype of $G\alpha_{13}$ -deficient embryonic fibroblasts. **(A)** Accumulation of inositol phosphates in the absence (open bars) and presence of thrombin (Thr., 1 U/ml), bradykinin (Bk, 100 nM), and LPA (100 nM) in cells from wild-type animals (left) and from $G\alpha_{13}$ -deficient animals (right). Shown are mean values of triplicates \pm SD (26). **(B)** Proliferation of wild-type and $G\alpha_{13}$ ($-/-$) cells in response to thrombin (1 U/ml), LPA (100 nM), and FCS (5% v/v). Shown are mean values of triplicates \pm SD (26). **(C)** Migration of serum-starved embryonic fibroblasts in response to thrombin (0.1 U/ml), LPA (50 nM), and fibronectin (Fn, 1 μ g/ml). Cell migration was examined with a blindwell microchamber (27). Numbers represent mean \pm SD ($n = 6$) of total cells per high-power field (200 \times).

DCP-1, a *Drosophila* Cell Death Protease Essential for Development

Zhiwei Song, Kimberly McCall, Hermann Steller*

Apoptosis, a form of cellular suicide, involves the activation of CED-3-related cysteine proteases (caspases). The regulation of caspases by apoptotic signals and the precise mechanism by which they kill the cell remain unknown. In *Drosophila*, different death-inducing stimuli induce the expression of the apoptotic activator *reaper*. Cell killing by *reaper* and two genetically linked apoptotic activators, *hid* and *grim*, requires caspase activity. A *Drosophila* caspase, named *Drosophila* caspase-1 (DCP-1), was identified and found to be structurally and biochemically similar to *Caenorhabditis elegans* CED-3. Loss of zygotic DCP-1 function in *Drosophila* caused larval lethality and melanotic tumors, showing that this gene is essential for normal development.

- mouse ES cell line Cj7 was done as described (19). Correctly targeted ES cell clones were injected into C57BL/6 blastocysts, and chimeras were bred with C57BL/6 and 129/Sv mice to generate heterozygous animals (19). Targeting of the α_{13} gene and germline transmission of the targeted allele were confirmed by Southern blotting. ES cell DNA or tail DNA from litters of F₁ were digested with Sma I and hybridized with the diagnostic probe from a 5' external upstream region, a 0.4-kb Sma I to Eco RI fragment.
23. Total RNA was purified from the embryo proper or from the yolk sac and reverse-transcribed with random primers and Moloney murine leukemia virus reverse transcriptase (Gibco BRL). Oligonucleotides used for PCR reaction were for α_{13} (AGCAGCG-CAAGTCCAAGGAGATCG and AGGAACACTCGA-GTCTCCACCATCC), α_{12} (TCAAGCAGATGCGC-ATCATCCACG and AACTCGCTTCTGCGGCTGA-AGGC), and α_{10} (GCCATGATCAGAGCGATGGA-CACG and CTGGGAAGTAGTCGACTAGGTGGG). Primer sequences were chosen so that primers hybridized to DNA regions encoded by different exons (7) in order to distinguish cDNA-dependent amplification from amplification of genomic DNA.
24. Whole mount immunohistostaining procedure was adapted from (20). Detergent was omitted from every step, and the entire procedure was performed at room temperature. Dissected yolk sacs were fixed in 4% paraformaldehyde, stored in methanol, and rehydrated before immunostaining. After incubation for 1 hour with dry milk (3% w/v), yolk sacs were incubated for another hour with anti-PECAM-1 (rat monoclonal antibody MEC 13.3, Pharmingen; 20 μ g/ml), washed, and incubated for about 40 min with alkaline phosphatase-conjugated goat anti-rat immunoglobulin G (Sigma). Yolk sacs were washed extensively, and color reaction was started by addition of 5-bromo-4-chloro-3-indoyl phosphate (BCIP) and nitro blue tetrazolium (NBT). The reaction was stopped after about 30 min.
25. Embryos were fixed in glutaraldehyde and OsO₄, embedded in Epon, sectioned at 0.5 μ m, and stained with toluidin blue.
26. Embryonic cells were prepared and cultured from E8.5 embryos as described (13). Inositol phosphate production and [³H]thymidine incorporation of serum-starved cells were determined as described (21).
27. For examination of cell migration, cells were serum-starved for 24 hours and migration was quantified by a microchamber technique. Cell suspensions (1 \times 10⁶ cells/ml) and stimuli were prepared in serum-free Dulbecco's minimum essential medium. Stimuli or control solutions (30 μ l) were placed in the lower compartment of a 48-well migration chamber (NeuroProbe). Wells were overlaid with a polycarbonate membrane (pore size, 8 μ m; NeuroProbe), and 50 μ l of cell suspension was added to the top well. Chambers were incubated for 16 hours at 37°C, then membranes were removed, fixed in methanol, and stained with hematoxylin. We quantified cells that had migrated through the filter by counting six nonoverlapping fields at 200 \times magnification. To determine whether the migration of cells in response to thrombin was chemotactic or chemokinetic, we performed checkerboard experiments (7). In the presence of a negative ligand gradient (higher concentration on the cellular site), there was still migration of cells on the upper site of the filter (about 60 to 70% compared to positive gradient conditions). Equal concentrations of thrombin on both sites resulted in cell migration comparable to that under a positive gradient, indicating that the observed migration was predominantly chemokinetic.
28. We thank J. Edens, Y.-H. Hu, and the La Jolla Cancer Research Foundation for technical assistance; T. Gridley for ES cell line Cj7; and A. Aragay, S. Pease, H. Wang, T. Wieland, and J. T. Yang for helpful suggestions. Supported by NIH grants GM 34236 and AG 12288 (M.I.S.). S.O. was a recipient of a fellowship from the Deutsche Forschungsgemeinschaft and the Guenther Foundation.

Programmed cell death, or apoptosis, is of fundamental importance for the elimination of cells that are no longer needed in an organism (1). During the past few years, there has been growing support for the idea that the basic molecular mechanism underlying apoptosis has been conserved during evolution among animals as diverse as nematodes, insects, and mammals (2). A central step in this cell suicide pathway is the activation of an unusual class of cysteine proteases, named caspases (3), that includes mammalian interleukin-1 β -converting enzyme (ICE) and the *ced-3* gene of nematodes (4). Caspases are synthesized as inactive zymogens that need to be processed to form active heterodimeric enzymes (4). However, the precise mechanism of caspase activation in response to apoptotic stimuli remains unknown. Likewise, with the exception of the *Caenorhabditis elegans* caspase CED-3, it is not clear what precise role any other caspase has in apoptosis.

The availability of many sophisticated genetic and molecular techniques makes *Drosophila* ideally suited for studying the questions of caspase activation and function. In *Drosophila*, like in mammalian systems, the onset of apoptosis is regulated by a number of distinct death-inducing stimuli (5). Genetic studies have led to the identification of three apoptotic activators, *reaper* (6), *head involution defective* (*hid*) (7), and *grim* (8), that appear to act as mediators between different signaling pathways and the cell death program. The deletion of all three genes blocks apoptosis in *Drosophila* (6), and overexpression of any one of them is sufficient to kill cells that would normally live (7–9). The products of these genes appear to activate one or more caspases, because cell killing by *reaper*, *hid*, and *grim* is

blocked by the baculovirus protein p35 (7–9), a specific inhibitor of caspases (10).

To gain further insight into the function and control of caspase activity, we isolated *Drosophila* caspase-like sequences. Degenerate oligonucleotides corresponding to two highly conserved regions flanking the active site of the enzyme were designed and used for a polymerase chain reaction (PCR) with a *Drosophila* 4- to 8-hour embryo cDNA library as the template (11). We obtained several PCR products of the expected size that were subcloned and sequenced (11). One clone was highly homologous to the region containing the caspase active site, including the highly conserved QACRG (12) pentapeptide. This clone was used to isolate full-length cDNA clones and to deduce the entire amino acid sequence of this putative caspase (11). The predicted open reading frame of the full-length cDNA encodes a protein of 323 amino acids (Fig. 1A). The DNA sequence surrounding the first ATG (CAAGATGACC) is in good agreement with the consensus sequence for translation initiation in *Drosophila* (13). The corresponding protein was named *Drosophila* caspase-1 (DCP-1). In comparison with other caspase family members (4, 14–16), DCP-1 is more homologous to CPP-32 and MCH-2 α than to ICE. It shares 37% sequence identity with both CPP-32 and MCH-2 α , 29% identity with NEDD-2 (ICH-1), 28% with CED-3, and 25% with human ICE. This sequence similarity suggests that DCP-1 may be a member of the *ced-3*–CPP-32 subfamily of caspases.

Caspases are synthesized as inactive proenzymes that are proteolytically processed to form the active heterodimer consisting of a p10 (10 kD) and a p20 (20 kD) subunit (4). The consensus sequence for proteolysis of many *ced-3*-like caspases is (D/E)XXD-Y (12), where X can be any amino acid and Y is a small amino acid, such as Ala, Gly, or Ser. Cleavage occurs

Howard Hughes Medical Institute, Department of Brain and Cognitive Sciences and Department of Biology, Massachusetts Institute of Technology, Cambridge, MA 02139, USA.

*To whom correspondence should be addressed.

9 September 1996; accepted 2 December 1996